Journal of VLSI Signal Processing 23, 267–280 (1999)

Realization of a Reaction-Diffusion CNN Algorithm for Locomotion Control in an Hexapode Robot

PAOLO ARENA AND LUIGI FORTUNA
Dipartimento Elettrico, Elettronico e Sistemistico, Universita' di Catania, V.le A.Doria 6, 95125, Catania, Italy

MARCO BRANCIFORTE
ST Microelectronics, R&D—Soft Computing Group, Stradale Primosole 50, 95100, Catania, Italy

Abstract. In this paper a reaction-diffusion CNN is implemented to generate and adaptively control locomotion in a biologically inspired walking robot. In particular a dedicated CNN development system has been realised to make the mechatronic device able to select, based on sensory stimuli, the most suitable locomotion type according to the environment. The first example of analog implementation of the biological paradigm of the Central Pattern Generator is therefore presented.

I. Introduction

Recently the technical and scientific community has been highly interested in life sciences, in particular in biology and neurobiology, since it was discovered that tasks like the adaptive generation and control of locomotion in legged walking robots required a high computational effort from a design, computating and implementation point of view. In fact it requires the concurrent generation and coordination of trajectories for all the robot leg joints. It can be easily understood that this effort tends to become unaffordable as the number of joints increase. This fact greatly encourages the construction of wheeled robots. But creatures do not walk through wheels: the legs are the results of natural evolution for clear reasons of adaptation to the most diverse ground conditions. Moreover even the simplest animals show distinct locomotion generation and control capabilities, even if a "brain" does not already exist. The continuous feedback between neurobiology, neurophysiology and engineering has therefore gone through a growing synergy: the investigation of animal behavior is not only interesting to solve a particular problem, (vision or locomotion), but also to understand the more interesting feature of how to build autonomous mechatronic devices, i.e. systems able to interact with the environment without needing remote control. Therefore, autonomy is viewed here as the capability to embed all the "intelligence" on board. Under this aspect the hardware implementation assumes a fundamental role. In fact, in this period, great attention has been given to find efficient algorithms to face with autonomous locomotion control. Several approaches have been recently focused. For example in [1] a biological approach has been focused to control motion in a insect-like structure. The solution typically involves in this case the use of an algorithm which has to be implemented in a digital traditional microprocessor. Moreover the choice of pneumatic actuators makes the degree of autonomy of the robot quite impossible. Among the other approaches, one of the outstanding solutions which have recently been receiving particular interest makes use of Artificial Neural Networks (ANNs), as confirmed by the attention of the main scientific ANN journals in the argument (see, for example [2]). Such structures have the powerful capability to approximate arbitrary non linear continuous mappings through efficient learning algorithms. Their bottleneck lies in the hardware implementation due to the massive connection among neurons. The Cellular Neural Network (CNN) paradigm [3] thorougly overcomes this problem since it is based on local interaction. The

lack of efficient learning strategies leads to the development of CNN algorithms based on trial and error techniques, or on the design of the dynamics of a single cell and the local connection strenghts. This last strategy has been the starting point for the work reported in this paper. In fact CNNs have been found to provide powerful architectures for modeling dynamics commonly met in living tissues [4]. These ones are characterized by the presence of a great number of locally and mutually interacting cells giving rise to complex spatio-temporal dynamics. Among the main phenomena encountered are auto waves and Turing patterns. The formers are spatio-temporal steady state oscillations taking place in active non-linear media (combustion and nerve waves are some examples) [5], while the latters are steady-state configurations characterized by spatial periodic patterns, like the animal coat patterns, which save their geometrical topology with the animal growth [6]. It has been demonstrated that both of these phenomena can be efficiently implemented in CNNs [7–9]. Since these phenomena are all solutions of the so-called reaction-diffusion partial differential equation (RD-PDE) structure, the CNNs able to reproduce them are called RD-CNNs [4]. In particular, in [9] the paradigm of the Central Pattern Generator (GPG), commonly used in neurobiology [10], has been suitably implemented into a RD-CNN in order to generate artificial locomotion in a ring-worm-like walking robot. Moreover, an hexapode walking robot has been introduced: the CNN hardware setup was able to generate the fast gait locomotion type and also to implement the transition between this type of gait and the swimming locomotion, by using the Turing pattern framework. In this paper this idea has been deeply investigated, and a CNN hardware board consisting in an array of 12×1 cells has been designed and realized together with all the circuits needed to connect the CNN to the legs of an hexapode walking robot, so as to implement in real-time all the main gait types of terrestrial insects: the fast, the medium and the slow gait. In fact these last two gaits are more complex than the first one, since they involve particular delays among the legs motions. It is here shown that all of them can be efficiently implemented in a CNN algorithm implemented in a hardware framework. Since the ciruits needed to connect the CNN cells to the robot legs are nothing more than a network of analog switches digitally driven, the whole hardware realized in this paper can be considered a particular development system to exploit the powerful capabilities of the RD-CNN to generate and control locomotion in biologically inspired walking robots. The possibility to have autowave and Turing patterns into the same CNN structure [11], and to have CNN analogic chips [12] opens the way to build efficient on-chip locomotion control strategies, the brain of the next generation autonomous robots.

II. The CNN Frame and the Realization of the CPG

In this section the model of the RD-CNN used to realize the locomotion control is briefly recalled. In particular firstly the paradigm of the CPG is presented and its implementation via a suitable CNN frame is introduced.

A. The CPG Scheme for Biological Locomotion

The Central Nervous System (CNS) produces specific patterns of motor neuron impulses during a coordinated motion. As in [13] we can define a motor program as "a set of muscle commands which are structured before a movement begins and which can be sent to the muscle with the correct timing so that the entire sequence is carried out in the absence of peripheral feedback."

The basic hypothesis is that the CPG, within the CNS, produces the basic motor programs [14]. Information derived from sensory inputs may modify the output of the pattern generator so as to adapt locomotion to the environment. More specifically, rhythmic movements that drive locomotion effectors (muscles) are triggered by a group of neurons, here called *Local Pattern Generating Neurons* (LPGNs). They in turn are controlled by a higher level neural center, called Centre of *Command Neurons* (CNs), which fixes a particular locomotion scheme based either on specific signals coming from the CNS, or on feedback deriving from sensory inputs. In such a way the output of the pattern generator can be modified so as to adapt locomotion to the environment [15, 16]. From a behavioral point of view, the whole locomotion system (CPG) therefore appears to be a complex activator-inhibitor system characterized by a hierarchical organization in which a group of neurons (the CNs), due to sensory or central excitations, activate other groups of neurons (the LPGNs) that generate the appropriate timing signals for the type of locomotion induced by the CNs. The whole system for locomotion generation can be therefore simply and schematically depicted in Fig. 1.

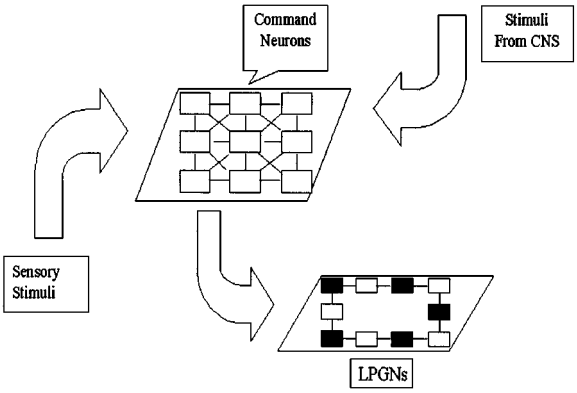

Figure 1. A scheme of the central pattern generator.

The CNs are a collection of cells which generate a specific pattern for each locomotion scheme. They are also responsible for the coordination between the LPGNs and the muscle system.

B. The CNN Structure

Several models of artificial neurons, resembling the structure and the dynamics of intermembrane chemical exchanges, have been introduced in literature. They are sometimes very complicated and their implementation would imply an excessive effort. Here the central hypothesis is that we want to implement an artificial neuron being always active, i.e. continuously generating action potentials. Therefore the model order can be reduced to that one of a second-order nonlinear oscillator. The generic cell structure in a $M \times N$ RD-CNN results to be [8]:

$$\dot{x}_{1,i,j} = -x_{1,i,j} + (1 + \mu + \epsilon)y_{1,i,j} - s_1 y_{2,i,j} + i_1; \tag{1}$$

$$\dot{x}_{2,i,j} = -x_{2,i,j} + s_2 y_{1,i,j} + (1 + \mu - \epsilon)y_{2,i,j} + i_2; \tag{2}$$

with

$$\begin{gathered} y_i = 0.5 \cdot (|x_i + 1| - |x_i - 1|) \\ i = 0, 1, \ldots, M-1, \quad j = 0, 1, \ldots, N-1 \end{gathered} \tag{3}$$

If such a cell is locally connected to its neighbors by means of a discretized diffusion template, already introduced in [4], we can derive the following RD-CNN with constant templates:

$$\dot{x}_{ij} = -x_{ij} + A * y_{ij} + B * u_{ij} + I \tag{4}$$

where $x_{ij} = [x_{1;i,j}\, x_{2;i,j}]'$, $y_{ij} = [y_{1;i,j}\, y_{2;i,j}]'$ and $u_{ij} = [u_{1;i,j}\, u_{2;i,j}]'$ are the state, the output and the input of the CNN respectively while A, B and I are the feedback, control and bias templates respectively. The cloning templates are:

$$A = \begin{pmatrix} A_{11} & A_{12} \\ A_{21} & A_{22} \end{pmatrix}; \quad B = 0; \quad I = \begin{pmatrix} i_1 \\ i_2 \end{pmatrix}; \tag{5}$$

where:

$$A_{11} = \begin{pmatrix} 0 & D_1 & 0 \\ D_1 & -4D_1 + \mu + \epsilon + 1 & D_1 \\ 0 & D_1 & 0 \end{pmatrix}; \tag{6}$$

$$A_{22} = \begin{pmatrix} 0 & D_2 & 0 \\ D_2 & -4D_2 + \mu - \epsilon + 1 & D_2 \\ 0 & D_2 & 0 \end{pmatrix}; \tag{7}$$

$$A_{12} = \begin{pmatrix} 0 & 0 & 0 \\ 0 & -s_1 & 0 \\ 0 & 0 & 0 \end{pmatrix}; \quad A_{21} = \begin{pmatrix} 0 & 0 & 0 \\ 0 & s_2 & 0 \\ 0 & 0 & 0 \end{pmatrix}. \tag{8}$$

Some theorems, proved in [7] and in [17] show that the above system, while used as a cell in a $M \times N$ CNN array, is able to show pattern formation or autonomous wave propagation for suitable choices of its parameters. In particular, if

$$\begin{gathered} \mu = 0.7, \quad \epsilon = 0, \quad s_1 = s_2 = s = 1, \\ i_1 = -0.3, \quad i_2 = 0.3 \end{gathered} \tag{9}$$

sufficient conditions are satisfied for this cell to show a steady-state dynamics consisting in a stable slow-fast limit cycle [7], while the corresponding RD-CNN generates autowaves. Moreover it holds:

$$D_1 = D_2 = 0.1 \tag{10}$$

and the so-called *Zero-Flux (Neumann)* boundary conditions [4] have been assumed.

In [9] the idea has been presented to implement the whole scheme of Fig. 1 by using RD-CNNs. In particular since CNs select the particular locomotion type from external stimuli, they can be efficiently realized by a RD-CNN showing Turing Patterns. Further, LPGNs, that generate the approriate command signals to trigger the muscle system, can be realized through RD-CNNs showing autowaves. The framework designed in [9] allows to see the command signals coming from the

CNs as a combination of binary signals which reflect the particular Turing pattern generated into the CNs. In [8, 9], the dynamics shown by Turing patterns and the possibility to obtain a particular steady-state configuration have been fully explained. Since these steady-state conditions, reflected by a particular Turing pattern, provide a network of binary signals, these ones can be used as command signals (resembling the outputs of the CNs) that allow suitable LPGNs configurations so as to actuate a given locomotion type. Therefore the CNs realization via RD-CNNs in the Turing pattern configuration will not be further discussed in this paper. From an experimental point of view, the focus is on the connections among the LPGNs and the actuator system as well as within the LPGNs themselves for each desired gait type.

III. The Gait Control in an Hexapode Walking Robot

The CPG introduced in the previous section is the most widely accepted biological locomotion scheme. It results to be a hierarchical system with several layers. The LPGNs represent a network of locally coupled neurons characterized by nonlinear oscillations. Each neuron can directly trigger the end effectors and at the same time "senses" local stimuli and is able to correct, via its local feedback, the motion of the associated mechanical part. Interleg coordination depends on the overall organization among the LPGNs under control of the CNs. A higher level control decides to adapt the global locomotion scheme to the environment. The locomotion control strategy reported in this paper aims to establish a new way to approach the problem by RD-CNNs, to provide local oscillations to the robot leg, which are "naturally" self-organized with the other legs. In this sense the interleg coordination problem is solved by the intrinsic structure of the approach. Sensors placed in the legs can affect the dynamics of the corresponding local triggering neurons according to the sensor signal that modifies the local oscillation dynamics so as to adapt the effector local motion. Moreover the local sensor signals do not affect the global behavior of the other LPGNs, since autowaves do not suffer from spurious reflections caused by such stimuli. Therefore the guidelines on how to modify the local oscillations depend on the characteristics of the particular sensor type and will not be discussed here. The strategy will provide an interesting and new methodological approach to implement the gait control in legged robots, fully open to every type of sensor and adaptable for each particular environment.

The prototype of the walking robot built in our laboratory to study and implement the strategy of locomotion control is the hexapode illustrated in Fig. 2. Each leg has two degrees of freedom and is moved by two servomotors: one drives the vertical position of the foot, while the other one drives the rotation of the leg to realize the locomotion steps. The kinematics have been designed so that both of the motions in each leg can be driven by the same output of one CNN cell, strictly resembling some biological cases where the same impulse triggers an ensemble of muscolar fibers which lead to a coordinated motion.

Among the different locomotion schemes that can be generated using this strategy [9], the attention is devoted in this subsection to a particular locomotion scheme, the gait, assumed to be imposed by either external stimuli or by specific commands from the CNS. Figure 3 depicts the various patterns of motion of insect legs with respect to the ground during the fast gait (Fig. 3(a)), the medium gait (Fig. 3(b)), and the slow one (Fig. 3(c)). Here each horizontal bar represents the time that each leg spends detached from ground (white part), or on ground (black part) [18]. The most common gait of insects is the fast gait Fig. 3(a). It is also called *alternating tripod*, since it is possible to distinguish two "tripods": $T_1 : \{L_1, R_2, L_3\}$ and $T_2 : \{R_1, L_2, R_3\}$. The legs belonging to each tripod are moved synchronously. In the fast gait configuration T_1 and T_2 are opposite in phase to one another. If the autowaves are considered in order to trigger the artificial insect legs in realizing this gait, the same autowave front, and therefore the state of one given cell (for instance C_1) will drive the tripod T_1, while another cell, showing an autowave front in opposing phase with C_1 will drive T_2. Roughly speaking, a particular Turing pattern, implemented by the CNs, imposes a particular locomotion type by sending the suitable binary commands, to connect the CNN showing autowaves (LPGNs) to the leg system. Indeed, the type of gait realized by insects is not only the "fast gait" depicted up to now, but also the "medium" and the "slow" gait, represented in Fig. 3(b) and (c). From this figure it can be realised that all gait types can be viewed as a modification of the basic fast gait, by a suitable modulation of the delay of each leg with respect to the other ones belonging to the same tripod. In fact the medium gait derives from the fast gait by introducing

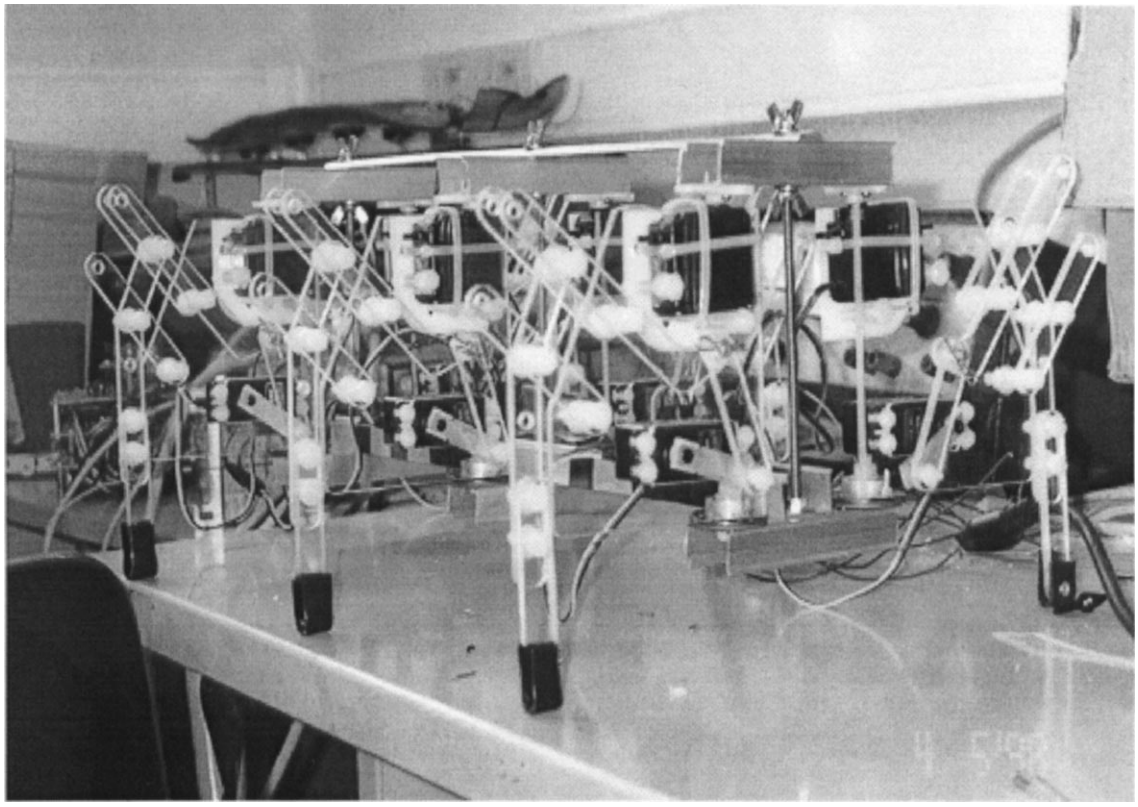

Figure 2. Hexapode walking robot prototype.

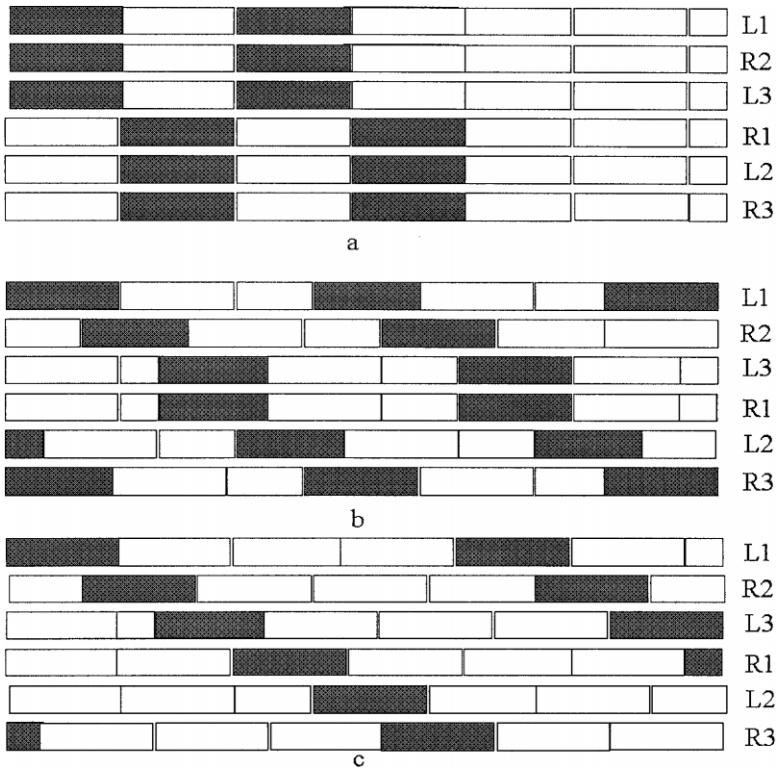

Figure 3. The three types of gait: a) fast; b) medium; c) slow.

a delay among the legs belonging to each tripod: R_2 has a phase lag with respect to L_1, and the same delay exists between L_3 and R_2. Similar considerations hold for the opposite tripod. Moreover the diagonally opposite legs couples, L_1 and R_3, and L_3 and R_1 proceed synchronously. When the phase delay involves also these two couples the slow gait sets on. Our aim is to establish a suitable strategy to connect the LPGNs among themselves and to the robot legs to realize all the types of locomotion shown in Fig. 3. This strategy represents the specific commands that the CNs send to the LPGNs to realize each locomotion type. It is apparent that in biology the spiking frequency of neurons cannot vary as a mere consequence of the walking speed. The hypothesis is that specific commands from other neural sites, coming from the central nervous system or directly from sensory feedback, can activate or inhibit specific connections in the LPGNs, giving rise to different pathways which eventually change the locomotion type. The scheme for locomotion control as designed and realized in this paper is depicted in Fig. 4. A CNN ring consisting of 12 cells is considered. Here suitable initial conditions lead to the onset of an autowave front, which, in steady-state conditions, proceeds with constant speed and unchanged amplitude periodically visiting all the cells. The connections among the state variables of the cells and the hexapode legs are also reported. For the fast gait configuration (dashed red lines), the alternating tripod requires that the legs of each tripode proceed in phase: therefore they have to be driven by the same cell, for example C_1. The other three legs must all be connected to another cell, for example to C_4. The further constraint to satisfy is that the two tripodes must be in an opposing phase. In this sense the reaction-diffusion mechanism plays a fundamental role: the self-adaptation of the phase among the cells. In fact, in the case at hand, if cell C_6 is directly connected to the cell C_1 in the sub-ring ($C_1 \rightarrow C_6$ through the path *a*), the diffusion process induces the autowave oscillation to take place in the cell C_1 directly after the cell C_6. A kind of phase rearrangement therefore takes place, in which cells C_1 and C_4 become in opposing phase to each other. The speed of the fast gait can be selected very easily, by choosing a particular sub-ring built of an even number of cells: of course, the more cells in the sub-ring, the slower the speed of this gait type. The medium gait (see Fig. 3(b)) is characterized by a constant phase delay among the three legs belonging to the same tripode, but the last leg of one tripode is in phase with the first one of the other tripode. Such

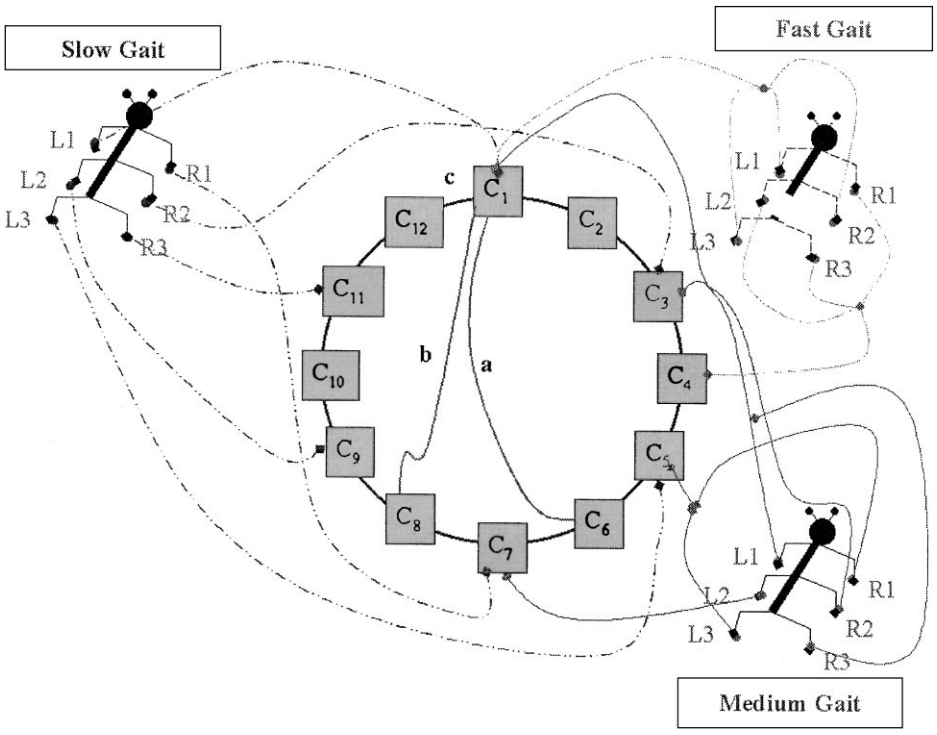

Figure 4. Connections between LPGN and the legs of the hexapode to realize the fast gait, the medium gait and the slow gait.

a configuration can be easily realised with the scheme of Fig. 4 by enhancing the path *b* and inhibiting *a* and *c*. The activation–inhibition of such paths is realised directly at the CNs level. The sub-ring with the connections to the robot legs depicted in solid lines, realizes this type of gait. Similar discussions lead to depict the slow gait, by comparing Fig. 3(c) with Fig. 4 where path *c* is allowed, *b* and *a* inhibited and therefore the whole ring of 12 cells is used (connection with the robot legs in dot–dot–dashed line). It should be noted that the transition among these types of gaits can be done in real time in the analog frame proposed, and the phase rearrangement among the cells is a function of the cell number.

IV. Design and Realization of the RD-CNN Framework

The strategy described in the previous sections has been implemented in a modular design. In this section all the phases of its realization are reported, from the design to the simulation and to the hardware implementation.

A. Design and Simulation

The first step consists in realizing the single CNN cell state Eq. (1), taking into consideration that:

- the approach just explained requires a CNN connected in a ring configuration;
- each CNN cell has to include the local influences from the neighboring cells, outlined by the template coefficients.

The double indexed cell state Eq. (1) can therefore be formulated as follows:

$$\dot{x}_{1,i} = -x_{1,i} + (1 + \mu + \epsilon)y_{1,i} - s_1 y_{2,i} + i_1 + D_1(y_{1,ip} - 2y_{1,i} + y_{1,if}); \tag{11}$$

The term $2D_1 y_{1,i}$ is due to the zero-flux boundary conditions. Moreover, $y_{1,if}$ and $y_{1,ip}$ represent the Laplacian effect deriving from the output of the previous cell ($y_{1,ip}$) and of the following one ($y_{1,if}$) with respect to the ith cell considered. In Fig. 5 the Op. Amp. at the

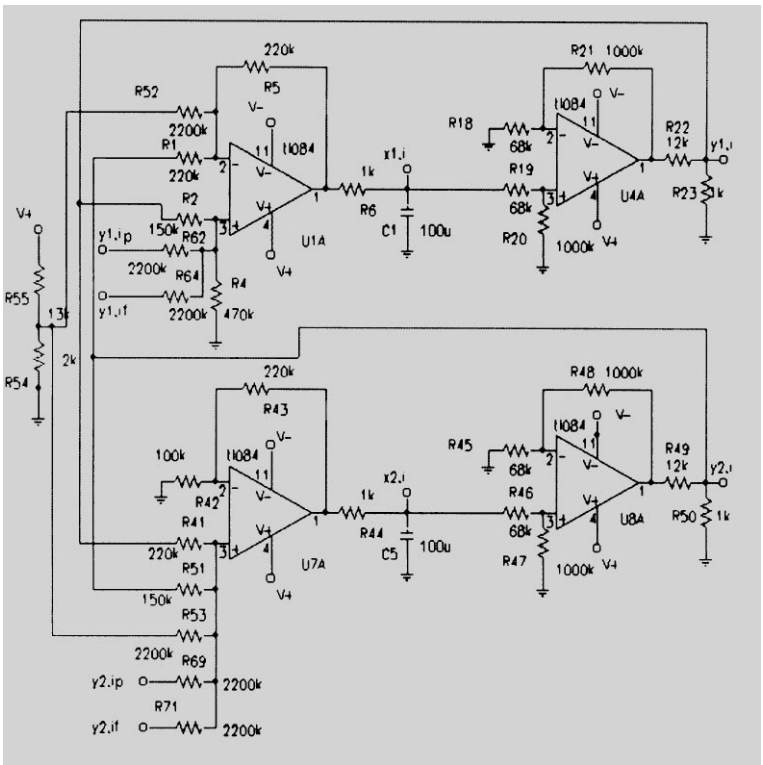

Figure 5. The whole cell circuit.

left top side realizes the following equation:

$$C_1 \cdot \frac{dx_{1,i}}{dt} = \frac{V_o - x_{1,i}}{R_6} \tag{12}$$

where

$$V_o = -\frac{R_5}{R_{52}} \cdot i - \frac{R_5}{R_1} \cdot y_{2,i} + \frac{R_5}{R_2} \cdot y_{1,i} + \frac{R_5}{R_{62}} \cdot y_{1,ip} + \frac{R_5}{R_{64}} \cdot y_{1,if} \tag{13}$$

which is formally identical to Eq. (11). In fact, by direct inspection it can be derived that Eq. (12) matches Eq. (11) if we divide both terms in Eq. (11) by 10^3 (this is to limit the currents into the circuit) and normalize with respect to time to take the introduction of the capacitor into account. The same strategy has been adopted to realize the second CNN cell state equation (implemented by the Op. Amp at the left bottom side of Fig. 5). Each of the two output non-linearities is simply realized by means of each of the two Op. Amp. depicted at the right hand side of Fig. 5. They exploit the natural saturation of an Op. Amp., whose output is further scaled to adapt the saturation levels to the desired values ± 1 V. Figure 5 depicts the whole cell circuit for the CNN ith cell, while Fig. 6 depicts the limit cycle associated with the two capacitor voltages of one cell (the state variables) (Fig. 6(b)) and the related currents (proportional the state variables derivatives) (Fig. 6(a)). It can be observed that the diffusion among the cell does not heavily alter the slow-fast characteristic of each cell oscillation. The slow dynamics can be clearly seen from Fig. 6(a), referring to the zone in the phase space around zero, that corresponds to the point ($x_1 = -2.8$ V; $x_2 = 1$ V) in Fig. 6(b). The sudden slope variations shown by currents in Fig. 6(a) give a clear idea of the slow-fast regime which characterizes the autowave propagation. Figure 7 and Fig. 8 depict the x_1 state variable by Spice simulation. Figure 7 refers to the 6 cells (C_1 to C_6) used to generate the fast gait. The period of each cell is about three seconds and the cell C_1 (magenta line) is opposit in phase with respect to C_4 (blue line). When the medium gait is selected, eight cells make-up the ring (Fig. 8). The period of each cell migrates to about four seconds, and C_1 is now in opposition of phase with C_5 (light blue line). This takes place via an enhancement of the slow dynamics with respect to the fast one. In fact the difference in dynamics of the same cell, when the number of cells in the ring is increased, lies only in the duration of the slow part of its oscillation, while the fast dynamics remains unchanged. Based on these considerations it can be concluded that in an array of many cells, a given cell in the slow dynamic range is indeed on its "edge of activity." This activity (the fast dynamic) is a function of the spatial diffusion process caused by the incoming autowave propagating from neighboring cells. This exactly matches all the simulations performed in earlier works [7, 19].

B. *Realization of the* 12×1 *RD-CNN for the Locomotion Control*

Figure 9 reports the whole 12×1 CNN cell realization. Referring to Fig. 4 it can be derived that in all the gait types the cells from C_1 to C_6 are always connected one to another: they form a fixed block that we'll call *Sub-Chain 1 (SC_1)*. The same holds for the sub-chain C_7 to C_8 (SC_2) and C_9 to C_{12} (SC_3). The connections among these three sub-chains are to be suitably connected to

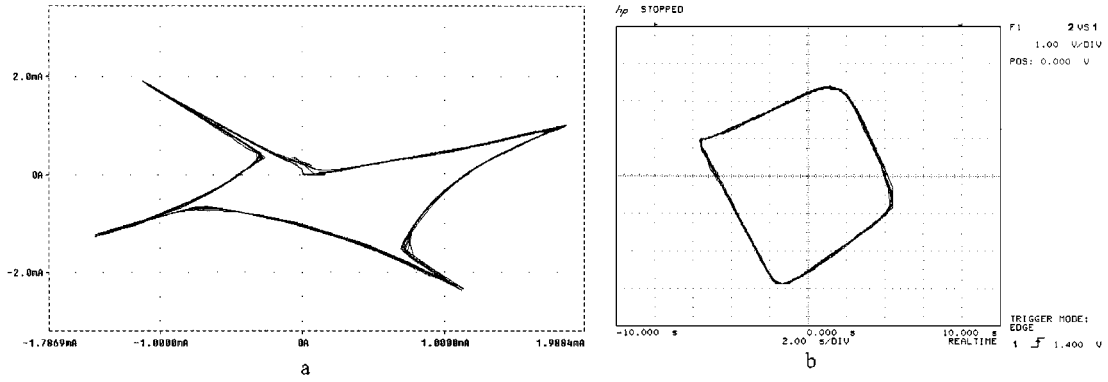

Figure 6. (a) Current limit cycle for a cell; (b) Voltage limit cycle for the same cell.

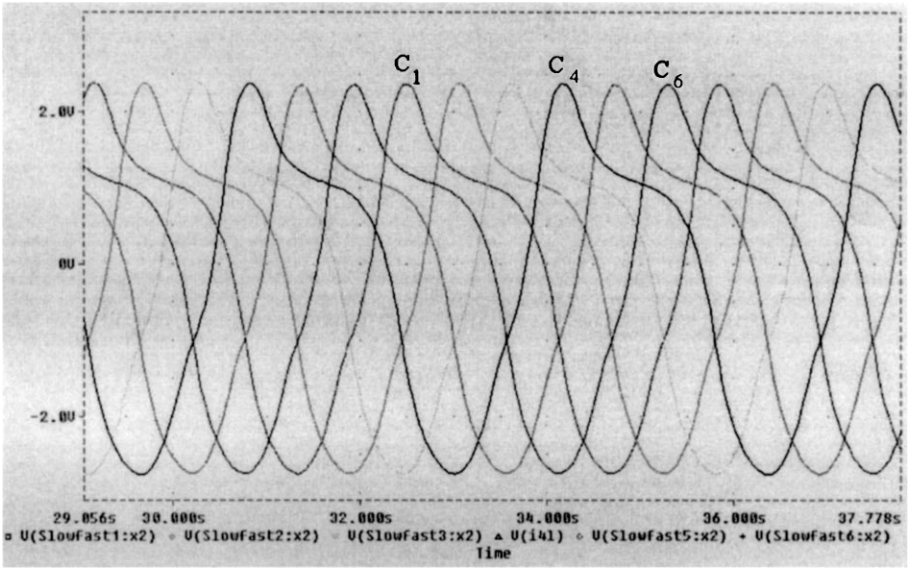

Figure 7. Temporal dynamics of the six cell CNN ring to generate the fast gait.

realize each type of gait as well as the transition among them. For example, to select the fast gait configuration the sub-chain SC_1 has to be closed within itself: the path "a" has therefore to be enhanced, while the "b" and "c" become inhibited (see Fig. 4). Similar conditions hold for the other two gait types. The hardware implementation of this scheme has been realized as schematically reported in Fig. 10. Here the three main blocks represent the three sub-chains introduced above, while the little boxes represent digitally driven analog switches, whose task is to realize the suitable connection among cells for each gait. Table 1 reports the connections among the cells of each sub-chain that have to be joint via the switches to realize each type of gait. For example, the fast gait requires that the first sub-chain must be closed within itself. In this case the cell C_1 follows cell C_6. Referring to the block SC_1 in Fig. 10, it means that the outputs of cell C_1(y_{11} and y_{21})

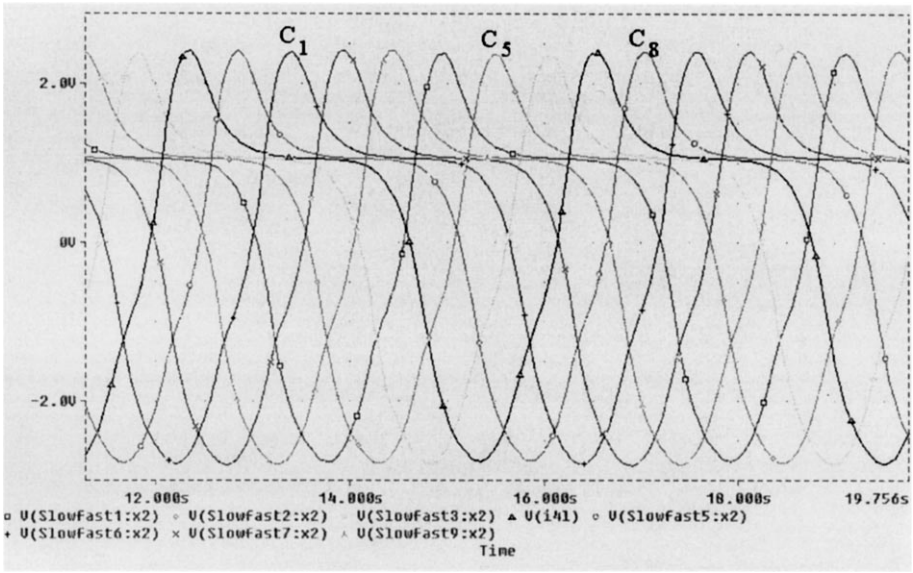

Figure 8. Temporal dynamics of the six cell CNN ring to generate the medium gait.

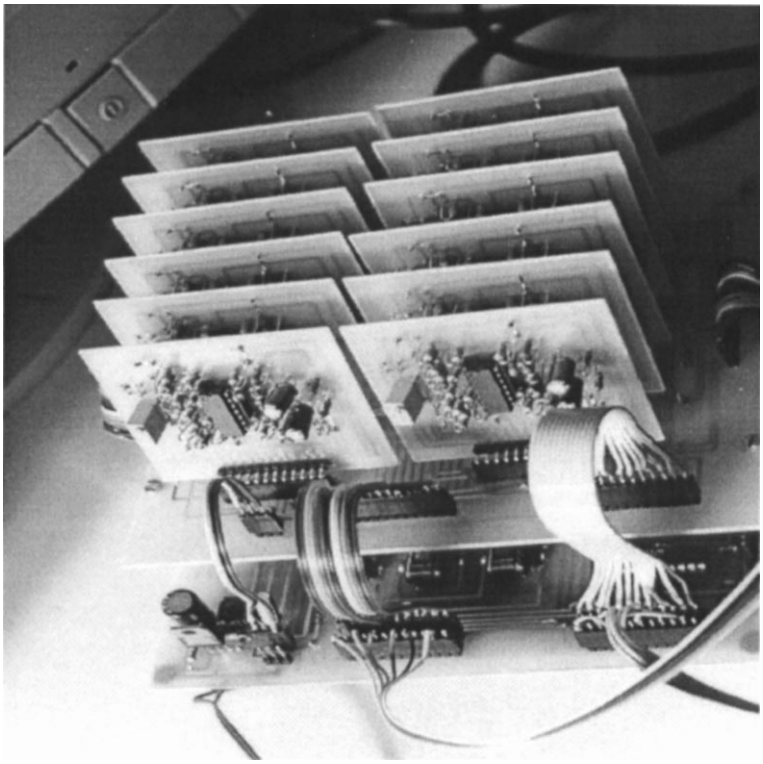

Figure 9. The 12 × 1 CNN setup.

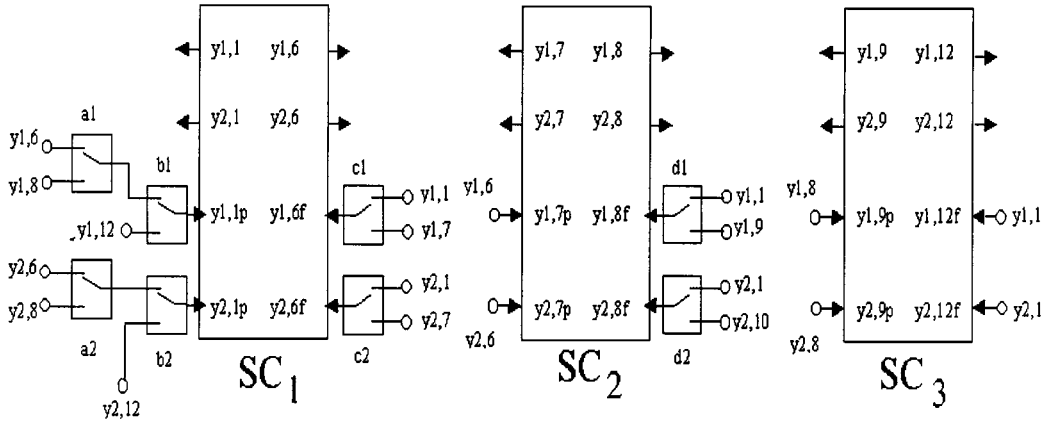

	b1-b2-d1-d2	a1-a2-c1-c2
Fast	H	H
Medium	H	L
Slow	L	L

Table 1

Figure 10. Design of the switching network among the different gaits.

have to be connected to $y_{1,6f}$ and $y_{2,6f}$, respectively, while the outputs y_{16} and y_{26} of cell C_6 have to be connected to $y_{1,1p}$ and $y_{2,1p}$, respectively. Therefore all the switches manipulating the outputs of SC_1 must be "high." Table 1 shows the corresponding position assumed by all the switches. Similar considerations can be made to realize all the other connections among the sub-chains: the corresponding switch configuration is reported in Table 1.

The last issue to be addressed involves the connections among each cell state variables and the robot legs to realize each of the gait types (see Fig. 4). These are depicted in Fig. 11, where, similarly to Fig. 10, the small boxes stand for switches, now connecting the robot legs to the corresponding cell state variables. The connections are summarized in Table 2. It has to be outlined that the analog switches, used for realising the connections among the sub-chains and the robot legs, are directly driven by the Command Neurons; these can be realised by using the Turing Pattern approach [9]. Figure 9 depicts the whole 12×1 CNN setup: the 12 cells are placed on a base board connecting them in a ring configuration, whose number of cells is decided by the switching network already discussed end implemented in a board placed just down the base board. This switching board is depicted in Fig. 12: here the simplicity of the circuits that realize the switching among the different gaits is clearly visible. The experimental measurements drawn from the already described board are reported through Fig. 13. It depicts the x_1 state variable for the cells C_1 and C_2 during the fast gait (Fig. 13(a)), the medium (Fig. 13(b)) and the slow gait (Fig. 13(c)), respectively. As already discussed in the previous section, the period of the slow-fast limit cycle for each cell depends on the number of cells connected to the ring. In particular, while the "fast" part of the limit cycle is unchanged (0.66 sec), if we measure the time interval between a maximum and the followimg minimum of the limit cycle which includes the "slow" part (i.e. distance in seconds between the vertical lines in Fig. 13(a–c)) it results 0.9 sec during the fast gait (connection of 6 cells), 1.08 sec during the medium gait (8 cells), and 1.8 sec during the slow gait (12 cells).

An efficient locomotion strategy has also to take the need for changes of direction into account. This can be very easily done by considering that each leg has a joint that allows the corresponding leg to rotate with respect to the body in order for the robot to move forward.

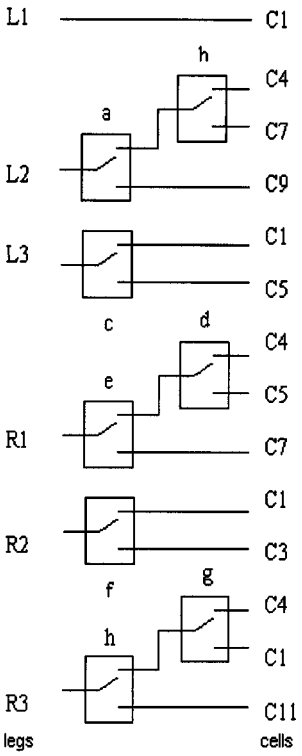

	a-d-g	b-c-e-f-h
Fast	H	H
Medium	H	L
Slow	L	L

Table 2

Figure 11. Design of the connections among the cells and the robot legs for each gait type.

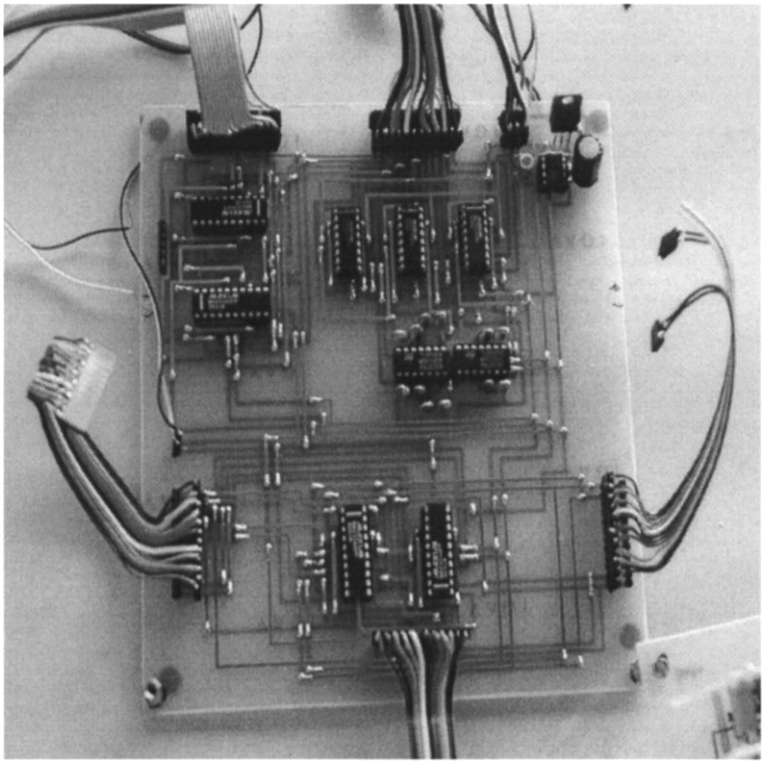

Figure 12. Board containing circuits that realize the switching among the different gaits.

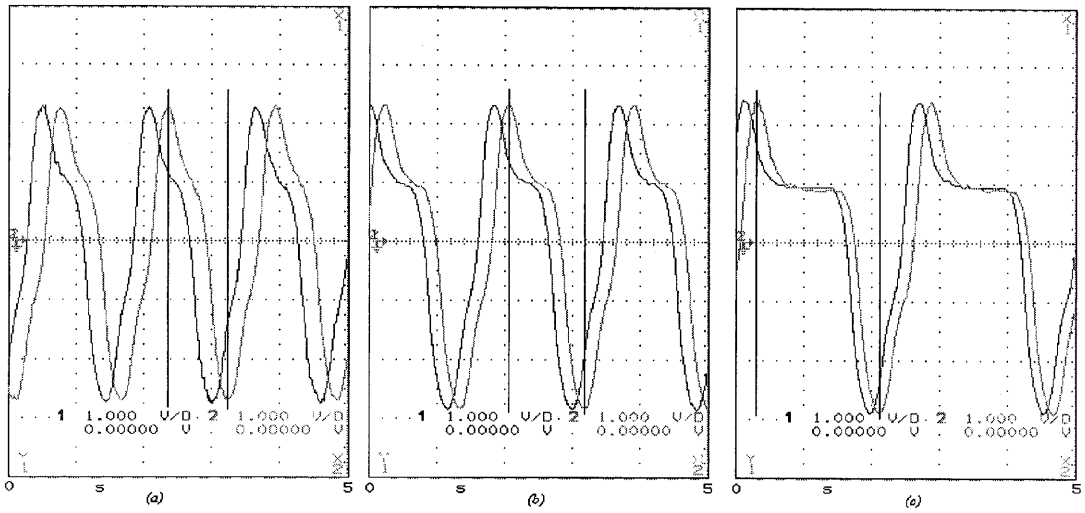

Figure 13. Experimental portraits of the cells state time dynamics for each gait type (see text).

For example in the fast gait configuration, each tripode has an ipsilateral couple of legs and a contralateral leg moving synchronously. If this unique contralateral leg is prevented from moving with respect to the others in the same tripode, this leg represents the fixed point of rotation for the robot. Therefore, it is sufficient to lock the robot "shoulder" of the middle right leg to perform a curve in the right direction. Of course, this can be performed as a consequence of the sensory feedback, in order, for example, to avoid obstacles. The whole strategy as depicted means to enhance the role of CNNs as powerful algorithms to generate complex spatio temporal dynamics including artificial locomotion. It is also to be outlined that the whole architecture configures as a particular hardware development system for the 12×1 CNN array, which therefore represents a simple analog implemetation of "brain for locomotion."

V. Conclusions

In this paper the role of CNNs as powerful devices to generate complex spatio-temporal dynamics is enhanced. The discrete component realization of a RD-CNN is presented to efficiently generate and control the locomotion in a biologically inspired walking robot. The strategy implemented allows the mechatronic device to be able to choose a particular locomotion type and to efficiently control the transition among three different types of gait. The whole frame is therefore a CNN development system which adaptively selects a locomotion type for the walking robot, based on local as well as global environmental feedback, provided by the sensors most suitable to the environment. The approach seems to be a very promising starting point towards the efficient realization of autonomous walking legged machines.

References

1. G.M. Nelson and R.D. Quinn, "Posture control in a cockroach-like robot," *IEEE Control Systems, Special Issue on Robotics and Automation*, Vol. 19, No. 2, April 1999.
2. Neural Networks, Vol. 11, 1998, Special Issue on robot control.
3. L.O. Chua and T. Roska, "The CNN Paradigm," *IEEE Trans. on Circuits and Systems—Part I*, Vol. 40, pp. 147–156, 1993.
4. L.O. Chua, M.Hasler, G.S. Moschytz, and J. Neirynck, "Autonomous cellular neural networks: A unified paradigm for pattern formation and active wave propagation," *IEEE Trans. on Circuits and Systems—Part I*, Vol. 42, No. 10, pp. 559–577, 1995.
5. V.I. Krinsky, "Autowaves: Results, Problems, Outlooks," in *Self-Organization: Autowaves and Structures Far from Equilibrium*, Springer-Verlag, Berlin, pp. 9–18, 1984.
6. L. Goras, L.O. Chua, and D.M.W. Leenaerts, "Turing patterns in CNNs—Part I: Once over lightly," *IEEE Trans. on Circuits and Systems—Part I*, Vol. 42, pp. 602–611, 1995.
7. P. Arena, S. Baglio, L. Fortuna, and G. Manganaro, "Self organization in a two-layer CNN," *IEEE Trans. on Circuits and Systems—Part I*, Vol. 45, No. 2, pp. 157–162, Feb. 1998.
8. P. Arena, M. Branciforte, and L. Fortuna, "A CNN based experimental frame for patterns and autowaves," *Int. J. on Circuit Theory and Appls*., Vol. 26, pp. 635–650, 1998.
9. P. Arena, L. Fortuna, and M. Branciforte, "Reaction-diffusion CNN algorithms to generate and control artificial locomotion," *IEEE Trans. on Circuits and Systems—part I*, Vol. 46, No. 2, pp. 253–260, Feb. 1999.
10. G.M. Shepherd, "Neurobiology" Oxford Univ. Press, third edition, 1994.
11. P. Arena, R. Caponetto, L. Fortuna, and L. Occhipinti, "Method and circuit for motion generation and control in an multi-actuator electro-mechanical system," European Patent No. 98830658.5, 30/10/98.
12. T. Roska and L.O. Chua, "The CNN universal machine: An analogic array computer," *IEEE Trans. on Circuits and Systems—Part II*, 40, 163–173, 1993.
13. C.D. Marsden, J.C. Rothwell, and B.L. Day, "The use of peripheral feedback in the control of movement," *Trends in Neurosci.*, Vol. 7, pp. 253–258, 1984.
14. D.M. Wilson, "Genetic and sensory mechanisms for locomotion and orientation in animals," *Am. Sci.*, Vol. 60, pp. 358–365, 1972.
15. P.S.G. Stein, "Motor systems, with specific reference to the control of locomotion," *Ann. Rev. Neurosci.*, pp. 61–81, 1978.
16. R.L. Calabrese, "Oscillation in motor pattern-generating networks," *Curr. Op. in Neurobiol.*, Vol. 5, pp. 816–823, 1995.
17. P. Arena, L. Fortuna, and G. Manganaro, "A CNN for pattern formation and active wave propagation," *European Conf. on Circuit Theory and Design, ECCTD '97*, Budapest, Aug. 1997.
18. G.K. Pearson, "The control of locomotion," *Sci. Am.*, Vol. 235, No. 6, pp. 72–86, 1976.
19. P. Arena, R. Caponetto, L. Fortuna, and G. Manganaro, "Cellular neural networks to explore complexity," *Soft Computing Research Journal*, Vol. 1, No. 3, pp. 120–136, Sept. 1997.

Paolo Arena was born in Catania, Italy, in 1966. He received the degree in Electronic Engineering and the Ph.D. in electrical engineering in 1990 and in 1994, respectively, from The University of Catania, Italy. Since 1996 he is Assistant Professor of System Theory. His research interest include adaptive and learning systems, neural networks, cellular neural networks, and collective behavior in living and artificial neural structures.
email: parena@dees.unict.it

Luigi Fortuna was born in Siracusa, Italy, in 1953. He received the electrical engineering degree from the University of Catania in 1977. Following graduation he joined the Dipartimento Elettrico, Elettronico e Sistemistico, where he is currently Professor of System Theory. In the period 1997–1999 he served as Associate Editor the IEEE Transaction on Circuits and Sistems. His research interest include system identification, control theory, cellular neural networks and chaotic circuits for criptography.
email: lfortuna@dees.unict.it

Marco Branciforte was born in 1968. He received the electronic engineering degree from the University of Catania in 1996. Following graduation he joined the International Institute of Vulcanology where he designed and built electronic circuits for remote sensing and vulcanological signal processing. He is currently with the ST Microelectronics, where he is a design engineer of electronic circuits for chaotic communications and for the implementation of Cellular Neural Networks.
email: marco.branciforte@st.com